Estimation of chlorophyll-a concentration in waters over the continental shelf of the Bay of Biscay: a comparison of remote sensing algorithms

Stéfani Novona

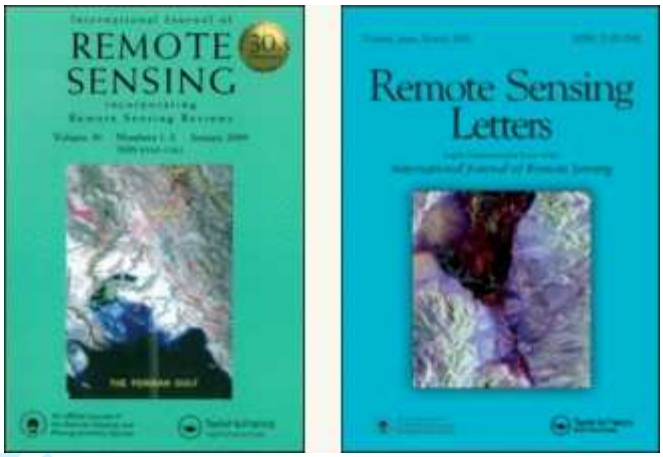

Estimation of chlorophyll-a concentration in waters over the continental shelf of the Bay of Biscay: a comparison of remote sensing algorithms

Journal:	*International Journal of Remote Sensing*
Manuscript ID:	TRES-PAP-2009-0140.R3
Manuscript Type:	Research Paper
Date Submitted by the Author:	
Complete List of Authors:	Novoa, Stéfani; AZTI-Tecnalia, Marine research division Chust, Guillem; AZTI-Tecnalia, Marine Research Division Valencia, Victoriano; AZTI-Tecnalia, Marine Research Division FROIDEFOND, JEAN; Centre National de la Recherche Scientifique (CNRS), Université Bordeaux-1 Morichon, Denis; Université de Pau et des Pays de l'Adour, Laboratoire de Sciences Appliquées au Génie Civil et Côtier
Keywords:	ALGORITHM, CHLOROPHYLL-A, REFLECTANCE, SPECTROMETER
Keywords (user defined):	

Estimation of chlorophyll-*a* concentration in waters over the continental shelf of the Bay of Biscay: a comparison of remote sensing algorithms

STÉFANI NOVOA*†, GUILLEM CHUST†, VICTORIANO VALENCIA†, JEAN-MARIE FROIDEFOND ‡, DENIS MORICHON§

† Marine Research Division, AZTI-Tecnalia, Sukarrieta, Spain

‡ UMR EPOC, Université Bordeaux 1, Talence Cedex (France).

§ Laboratoire de Sciences Appliquées au Génie Civil et Côtier, Université de Pau et des Pays de l'Adour, Anglet, France

Abstract

Ocean colour imagery is used increasingly as a tool to assess water quality via chlorophyll-*a* concentration estimations in European waters. The Bay of Biscay is affected by major river discharges, which alter the constituents of the marine waters. Chlorophyll-*a* algorithms, designed for use at global scales, are less accurate due to the variability of optically-active in-water constituents. Hence, regionally-parameterized empirical algorithms are necessary. The main objective of the present study was to develop a regional algorithm to retrieve chlorophyll-*a* concentration (Chla) in surface water using *in-situ* Remote Sensing Reflectance (Rrs), for a subsequent application to MERIS satellite images. To address this objective, a platform was developed initially and a measurement procedure adapted for the field HR4000CG Spectrometer. Subsequently, the procedure was tested during a survey over the southeastern Bay of Biscay (North-East Atlantic Ocean), to establish a MERIS Chla algorithm for the area, by comparing different global remote sensing Chla algorithms, with band ratios. Results validated with the jackknife resampling procedure show a satisfactory relationship between the 510/560 nm Rrs ratio (r^2_{jac} = 0.681). This ratio is better correlated to Chla than those obtained with established Chla remote sensing algorithms. High content in coloured dissolved organic matter (CDOM>0.4 m^{-1}) and suspended particulate matter (SPM>2.8 $mg.l^{-1}$) influenced this relationship, with yellow substances having a stronger effect.

1. Introduction

Since the publication of the Water Framework Directive (WFD, 2000/60/EC) and the European Marine Strategy Framework Directive (MSFD, 2008/56/EC), quality assessment of European waters has become a major institutional issue, as its application will require an adequate monitoring of water elements. The MSFD strategy aims to "promote the sustainable use of the seas and conserve marine ecosystems'' and increases the extension of marine waters that need to be protected to 200 nautical miles (including the water column, the sea bed and its sub-surface geology; Borja, 2006). Therefore, the implementation of this directive, requires an intense and continuous monitoring of water bodies, for which the application and development of new tools and technologies is essential.

One of the biological water constituents to be assessed is phytoplankton biomass (Devlin *et al*. 2007, Domingues *et al*. 2008, Revilla *et al*. 2009), which is estimated through chlorophyll-*a* concentration (hereinafter referred to as Chla). This parameter is a good indicator of eutrophication risk, which is considered as one of the major environmental problems across Europe (Bøgestrand *et al*. 2005). Ocean colour imagery is used increasingly as a monitoring

*Corresponding author. Email address: snovoa@azti.es

tool, to complete the data sets collected by *in-situ* measurements of different water parameters such as Chla (Gohin *et al*. 2008, Hellweger *et al.* 2004). For instance, optical satellite sensors such as SeaWiFS (Sea-viewing Wide Field-of-view Sensor) and MODIS (Moderate-Resolution Imaging Spectroradiometer) provide global and daily ocean colour information (http://oceancolour.gsfc.nasa.gov/). Satellite-derived Chla maps are a key data source to study the distribution pattern of organisms and nutrients (Guillaud *et al*. 2008), for harmful algal blooms monitoring (Miller *et al*. 2006) and for fisheries research (e.g. Zainuddin *et al*. 2006), amongst other applications.

The colour of the water is established by the scattering and absorption of visible light by pure water, together with inorganic and organic, particulate and dissolved material present in the medium. From an optical perspective, three main components affect the properties of water bodies: 1) phytoplankton and other microscopic organisms; 2) suspended inorganic material (SPM); 3) yellow substances or coloured dissolved organic matter (CDOM), which includes also detrital particulate material (IOCCG 2000). A marine water classification was first introduced by Morel and Prieur (1977), which partitioned waters into Case 1 and Case 2.They suggested the use of high or low values of the ratio of pigment concentration to scattering coefficient as a basis for differentiating between Case 1 and Case 2 waters. Nonetheless, their concept has evolved over time and the definition is not standardised (Gordon and Morel 1983, Prieur and Sathyendranath 1981, Morel 1988, IOCCG 2000, Lee and Hu 2006, see review Mobley *et al.,* 2004). In general, and according to the International Ocean-Colour Coordinating Group (IOCCG 2000), Case 1 waters are those in which phytoplankton (with their associated and co-varying retinue of material of biological origin) is the main element altering the optical properties of the water. All the optical properties of Case 1 waters can be modelled as a function of chlorophyll-a concentration. On the other hand, Case 2 waters are affected not only by phytoplankton and associated substances, but also by other suspended inorganic particles and yellow substances that vary independently of phytoplankton, needing to be considered as independent variables.

Water constituents are also region-specific due to the intrinsic variability of these optically-active substances, because of factors such as river input (e.g. suspended matter type and grain size) and phytoplankton composition (Carder *et al*. 1999). The absorption of light by Chlorophyll-*a* and its auxiliary pigments can also vary with phytoplankton species as well as the physiological state of the cells (Morel *et al*. 1993). Algorithms designed for use at global scales have been shown to be less accurate in Case 2 and continental shelf waters (Morel and Prieur 1977), because of this variability (Carder *et al.* 1991, Darecki and Stramski 2003). For that reason, the development of regionally-parameterized algorithms is needed, to better assess water quality (IOCCG 2000). The calibration and validation of ocean colour remote sensing data requires accurate field determinations of the water-leaving radiance signal (Mobley 1994). Hence, in order to interpret satellite imagery in specific coastal waters, empirical relationships between the parameters of interest and *in-situ* optical measurements need to be estimated (Doxaran *et al*. 2002, Froidefond *et al*. 2002, Ouillon and Petrenko 2005, Gitelson *et al*. 2008, and Petus *et al*. 2008). These empirical relationships are used then to establish empirical algorithms. In addition to band ratios and combinations, several other methods have been used to map chlorophyll-a concentration in surface waters. For example, model-based approaches (Carder *et al.* 1999) are used to generate sets of simulated spectra for given ranges of concentrations for different components; and principal components approaches are used to establish very simple and stable algorithms that can be implemented very rapidly (Sathyendranath *et al.* 1994). Also, a more sophisticated and expensive approach is the one employed by Schiller and Doerffer (1999), who developed a Case 2 chlorophyll-a algorithm with neural networks.

The main objective of the present study was to develop a regional algorithm to retrieve Chla in surface water using *in-situ* Remote Sensing Reflectance (Rrs), for a subsequent application to MERIS satellite images. To address this objective, a platform was developed initially and a measurement procedure adapted for the field High-Resolution Fiber Optic Spectrometer HR4000CG (Ocean Optics, Inc. 2001-2006). *In-situ* spectral signatures were acquired for later calculation of Rrs. The measurement procedure was established in the laboratory and in the field. Subsequently, the procedure established was tested during a survey over the southeastern Bay of Biscay (North-East Atlantic Ocean), to establish a MERIS Chla algorithm for the area, by comparing different global remote sensing Chla algorithms, with band ratios.

2. Estimation of remote sensing reflectance

Rrs estimation provides an essential connection between imagery from satellite sensors and *in-situ* concentrations of water constituents (Gordon and Morel 1983, O'Reilly *et al*. 1998). Rrs is a parameter that indicates the effective reflectance of a body of water when viewed by a remote sensor; it is used to derive biophysical parameters such as Chla. Rrs is defined as the ratio of water-leaving radiance L_w measured above the water surface, to the incident downwelling irradiance E_d just above the water surface. Rrs is expressed as (Mobley 1999):

$$\text{Rrs}\,(0^+,\lambda) = \frac{L_w(0^+,\lambda)}{E_d(0^+,\lambda)} \qquad (1)$$

The water-leaving radiance L_w cannot be measured directly with an instrument; instead, the upwelling radiance L_u (λ) is measured just above (0^+) or just below (0^-) the air-water interface. For measurements above the water surface, the radiance measured when the sensor views the sky (L_{sky}) and the reflected sky radiance when the spectrometer views the sea surface (L_u) need to be taken into account. These two parameters are related, through the reflectance factor ρ, a complex factor that depends on incident light, viewing directions, wavelength, wind speed and cloud coverage (Mobley 1999). Thus, the water-leaving radiance above the water surface (L_w) is equal to $L_u - L_{sky} * \rho$.

When the sensor is placed below the water surface, the conversion of the upwelling radiance into water-leaving radiance is performed by taking into account the variation of the refraction index of water in relation to the air *n* (1.33 for freshwater and 1.34 for seawater) and the radiance transmittance *t* (0.98 for a sensor pointing towards the nadir) at the water-air interface (Mobley 1999). Therefore, to obtain water-leaving radiance L_w (λ), the upwelling radiance L_u is multiplied by the conversion factor t/n^2.

The index of refraction changes when the sensor is placed below the water surface, since the spectrometer was calibrated for air measurements. In the water, the semi-opening angle (θ_{water}) is different and is given by the Descartes´ law:

$$\theta_{water} = \arcsin\,[(1/n) * \sin\theta_{air}] \qquad (2)$$

The solid angle (angle in three-dimensional space) corresponding to a measurement performed with a 4º semi-opening angle in the air ($\Omega IFOV = 2\pi(1-\cos\theta)$, corresponds to 1.53×10^{-2} steradians, whereas in seawater it is of 0.85×10^{-2} and in freshwater it is 0.66×10^{-2}. This results in an angle decrease by a factor of 1.796 for seawater (Froidefond and Ouillon 2005) and

1.770 for freshwater. Therefore, this factor multiplied by the t/n^2 factor, results in a multiplication factor of 0.98 for the L_u measurements acquired in both media.

The downwelling radiance L_d is measured directly when the sensor views a Lambertian Spectralon plate and is kept pointing in the same direction as for the upwelling radiance. The E_d downwelling irradiance can be then calculated, by taking into account the known irradiance reflectance of the Lambertian surface R_g (Labsphere WS-1 Diffuse Reflectance Standard = 0.99) as follows (Doxaran *et al*. 2002):

$$E_d = \pi \frac{1}{R_g(\lambda)} L_d(\lambda) \qquad (3)$$

3. Instrumentation

Radiance measurements were obtained using an Ocean Optics High-Resolution Fiber Optic Spectrometer HR4000CG (Ocean Optics, Inc. 2001-2006). This device measures radiance (expressed in relative intensity units, i.e. digital counts; Dall'Olmo and Gitelson 2005) between 200 to 1100 nm in 3648 channels, with a spectral resolution of 0.75 nm (FWHM: Full Width at Half Maximum). The HR4000CG spectrometer is connected to a computer via USB, from which it draws power. Data are stored into a memory chip on the HR4000CG spectrometer, processed by the Ocean Optics operating software Spectrasuite (www.oceanoptics.com/Products/spectrasuite.asp) (Ocean Optics Inc. 1999-2007). The spectrometer is connected then to a Gershun tube (http://www.oceanoptics.com/Products/gerkit.asp) of an 8º field-of-view, by means of a 20 m-long optical fibre. The calibration of the device was performed in the factory, which provided a calibration certification data sheet.

To measure the upwelling radiance (L_u) of water surface in the field, a stainless steel flotation device was developed, to mount the sensor (Figure 1); this was based mainly upon the mini-catamaran platform implemented by Froidefond and Ouillon (2005). Its dimensions are 50 x 50 x 15 cm, with a weight of approx. 8 kg. The dimensions were selected in order to minimize its influence on the optical measurement, whilst the symmetrical square shape avoids the anisotropic influence of its shade. This device enables the measurements to be taken far from the ship and, therefore, away from its shade. With this prototype, the Gershun tube is maintained approximately 1 cm below the water surface (under calm sea conditions), permitting upwelling radiance measurements below the surface and away from any shade-producing objects, except for the flotation device.

(*Approximate location of Figure 1)

The downwelling radiance (L_d) was measured on a Labsphere Spectralon® (www.labsphere.com) target, which was placed on a stand designed to measure the irradiance at nadir (90°). The Gershun tube was pointing directly towards the target (perpendicularly) and the stand was placed facing the sun for the downwelling radiance measurement. The Gershun tube was placed on the platform approximately 6 cm, perpendicularly, above the Spectralon target.

The measurements in the field were performed quasi-simultaneously. Firstly, the L_d was measured on the Spectralon target and within the next 5 to 10 minutes, the same sensor was placed on the floating platform to measure the upwelling radiance L_u.

4. Measurement procedure

In order to establish a sampling procedure for the HR4000CG spectrometer, several experiments were performed to determine the optimal parameters and conditions for the measurements.

Sun glint, i.e. the specular reflection of sunlight off the sea surface, affects the correct acquisition of spectral information concerning in-water constituents. This effect can be highly mitigated by measuring water-leaving radiance below the water surface (Froidefond and Ouillon 2005). For that reason, an experiment was carried out to estimate the difference between measurements performed above and below the water surface, using the protocol established by Froidefond and Ouillon (2005), for the TriOS radiance/irradiance sensors as a reference. Upwelling radiance was measured by placing the Gershun tube directly (1 cm) above and (1 cm) below the water surface, pointing towards the nadir. The experiment was performed in a dark room, with a 100 watt light bulb as the only source of light; with the sensor pointing at a 50º angle. This was the optimal angle, in order not to have shade produced by the Gershun tube. At the bottom of the container filled with water, white paper was placed to obtain significant radiance intensity. Approximately, 20 scans were performed for each experiment undertaken in the laboratory. Radiance measurements above and below the water surface presented analogous spectral curves, in agreement with Froidefond and Ouillon's (2005) study. In our experiment, an absolute difference of 4.1% on average, was found between the 200 and 1100 nm wavelength range. In addition, the Kurskal-Wallis test performed for the spectral region of maximal radiance differences (650 nm) did not show any significant difference between the medians (P-value = 0.14).

Integration-time is the time over which the sensor monitors incoming light (photons). The integration-time needs to be adjusted, such that the greatest amount of light that is anticipated for the application selected causes a signal of about 85% of the spectrometer's capability (Ocean Optics Inc. 1999-2007). The light intensity determines the integration-time needed to be adjusted in every experiment. Tests performed in the laboratory and field pre-established an integration-time of 0.3 seconds for downwelling radiance measurements (i.e. on Spectralon®) and of 1 second for upwelling radiance measurements (i.e. target, mainly for water surface). These settings were modified eventually in accordance with the specific environmental conditions of each measurement. For example, the integration time was decreased when the light intensity was too high; to avoid signal saturation; it increased when light intensity was too low, in order to reach 85% of the spectrometer capability.

In order to obtain accurate spectral radiance data, the inherent noise in the instrument (i.e. background electronic noise caused by the power supply) needs to be removed. With this requirement, in addition to the conventional subtraction of the dark spectrum (measured under dark conditions) (Dall'Olmo and Gitelson 2005), the electric dark correction was applied to both upwelling and downwelling irradiance measurements. This correction enables a dark-level correction during temperature changes caused by the power supply (Ocean Optics, Inc. 2001-2006).

Smoothing is an additional way of reducing noise in the data and reveal the important underlying shape of the spectral signature. The simplest form of smoothing is the "moving average", or "moving box". The boxcar smoothing parameter allows for the setting at the width of an averaging box, which substitutes each data value with the average of adjacent channel values. The greater the smoothing width, the smoother the data and the higher the signal-to-noise ratio (S:N). Tests performed in the laboratory and field pre-established a boxcar smoothing of 6 to 8, as a good compromise between the loss of information and the reduction of

noise. The spectra obtained were additionally smoothed to a resolution of 5 nm, as to remove high-frequency noise (Dall'Olmo *et al.* 2005).

The discrete spectral acquisitions were stored individually, in order to remove spectral observations that were distant from the rest of the spectra (for example, affected by accidental shade caused by the movement of the vessel). The percentage deviation of each spectrum with respect to the mean, was calculated and the spectra with a deviation higher than 10% were removed.

5. Case study: Bay of Biscay

5.1. Study area

The Bay of Biscay is located between latitudes 43.5° and 48.5° N and between longitudes 2° and 8° W. It is an open embayment, where the Spanish coast is in the southern part with an orientation West-East and the French coast in the eastern part oriented Southeast-Northwest (Figure 2). The bay is physically and hydrologically complex; it is characterized by strong climatic and seasonal variations and spatio-temporal heterogeneity (González *et al*. 2004). The continental shelf of the Bay of Biscay receives freshwater inputs from three main watersheds on the French coast and several smaller rivers on the Spanish coast. The mean annual river flows for the Loire, the Gironde and Adour are of 835 $m^3.s^{-1}$ (Guillaud *et al*. 2008), 989 $m^3.s^{-1}$ (Doxaran *et al*. 2009), and 300 $m^3.s^{-1}$(Petus *et al*. 2008), respectively. Numerous rivers on the northern coast of Spain discharge around 350 $m^3.s^{-1}$ per year (Cantabrian Hydrographical Confederation 2009). The annual cycle of phytoplankton in the Bay of Biscay is typical of a temperate sea, i.e. there is a mixing period during winter time followed by a stratification phase in the summer (Longhurst 1998), whilst phytoplankton blooms occur during the transition periods (spring and autumn). Chlorophyll-*a* concentrations can reach 16 $\mu g.l^{-1}$ in transitional waters (Gohin *et al.* 2008, Borja *et al*. 2004), 8 $\mu g.l^{-1}$ in coastal waters (Borja *et al*. 2004) and 3 $\mu g.l^{-1}$ in oceanic waters (García-Soto and Pingree 2009). The phytoplankton dynamics at a regional and local scale are influenced also by the intrusion of saline waters (originating in Azores) during winter-spring, the upwelling pulses during the summer, and by river discharge and water turbidity (Varela 1996, Orive *et al*. 2004). The month of May was selected for the experiments because: 1) chlorophyll-*a* peaks take place during spring (Garcia-Soto and Pingree 2009); 2) the daylight hours are long (approximately 15 hours), allowing more time for measurements; and 3) there is a higher possibility of cloud-free satellite images (less rain between May and September; Pérez Puebla 2009).

(*Approximate location of Figure 2)

5.2. Oceanographic survey

In May 2008, spectral and biogeochemical measurements were performed during a 20-day survey over the continental shelf of the Bay of Biscay (Bioman 2008 Campaign) on board the "*Investigador*" vessel. Sixty-eight stations were sampled, with the aim of obtaining spectral signatures along a Chla gradient. Measurements were undertaken mainly near the sea surface, between 9:00 and 17:00 (GMT), at water depths of between 20 and 1962 meters: hence, within the boundaries of the continental shelf of the Bay of Biscay. Measurements were performed on the side of the ship where no shade was present at the time. Figure 2 shows the location of the sampling stations. Around 100 L_d and L_u scans were performed, per station. Thirty-five of the measurements were performed under clear sky conditions with broad sunshine, 12 under

completely covered skies and 22 under intermediate conditions (scattered clouds). The water samples were taken at the sea surface, within 10 minutes of the spectral measurements.

At each sampling station, surface temperature (ºC) and salinity were measured with a thermosalinometer. Turbidity was also measured *in-situ* by nephelometry (Nephelometric Turbidity Units, NTU), with a HANNA portable turbidimeter with a measuring range between 0.01 and 1000 NTU (Nephelometric Turbidity Unit) and an accuracy of ± 2% of the measured value. The chlorophyll-*a* and suspended particulate matter concentration (SPM) were measured at the sea surface, by filtration of 1-2 l of water at each station, using Whatman® GF/C filters with a diameter of 47 mm and a porosity of 1.2 µm. Filters were frozen (-20°C) immediately and taken to the AZTI Marine Research Centre, where Chla was determined by spectrophotometry (following the Jeffrey and Humphrey (1975) protocols) and SPM was estimated by gravimetry (following the APHA-AWWA-WPCF (1989) protocols). Filtered water was saved in the refrigerator for later analysis of coloured dissolved organic matter concentration (CDOM) in the laboratory, by means of spectrophotometry. The colour of the water samples was estimated against MilliQ distilled water, at a wavelength of 460 nm. Most of the biogeochemical sampling and optical determinations were undertaken quasi-simultaneously. The reflectance measurements were acquired with a HR4000CG spectrometer using the protocol described in the previous section.

5.3. Chla estimation

Band ratios between different wavelengths are used in satellite imagery to determine chlorophyll concentrations in open waters (O'Reilly *et al*. 1998). The presence of phytoplankton highly decreases the reflectance in the blue region of the spectrum, whilst it does not significantly affect the green reflectance. Hence, ratios of two reflectances, one in the blue and the other in the green, are used as a technique to relate reflectances with in-water constituents. The ratio "blue-to-green" technique, where $R(\lambda_1)/R(\lambda_2)$ (λ_1=443, 490, and 510 nm; λ_2 = 550, 555, and 560), is used as a way to deal with the variability and the uncertainty affecting the absolute reflectance and water-leaving radiance values (O'Reilly *et al*. 1998). The ratio values systematically decrease with increasing Chla. The OC4 algorithm used for SeaWiFS sensor takes the greater of the three ratios Rrs(443)/Rrs(555), Rrs(490)/Rrs(555), Rrs(510)/Rrs(555) values; the MERIS (Medium Resolution Imaging Spectrometer Instrument) algorithm OC4E takes the greatest of the three ratios Rrs(443)/Rrs(560), Rrs(490)/Rrs(560), Rrs(510)/Rrs(560), whilst MODIS algorithm OC3M uses only the greatest of the two ratios Rrs(443)/Rrs(550), Rrs(490)/Rrs(550) (O'Reilly *et al.* 1998). This means that the maximum band ratio is calculated for each pixel in an image to provide an estimate of Chla. The MODIS chlor_a_3 algorithm, developed by Carder *et al*. (1999), only uses the Rrs(443)/Rrs(551) and Rrs(488)/Rrs(551) ratio.

Therefore, log-transformed ratios used in the algorithms were calculated for the Bay of Biscay dataset and compared with log-transformed Chla to determine the relationship between these parameters (Table 1). In addition to the band ratio calculations, the previously mentioned algorithms were applied to our dataset (Table 2), as well as the OC4E algorithm adjusted to our dataset (i.e. our own coefficients for the equation). Using the R program, a model was established between the log-transformed Chla concentrations, using the maximum reflectance value for each station. The resulting algorithms were validated with the jackknife resampling procedure (Burnham and Anderson 2002), developed with R language (Venables and Smith 2007). With a data set of *n* data stations, the jackknife procedure recalculated the model *n* times, leaving out one station in turn. Each one of the regression models, based on the *n*-1 times station, was then applied to that excluded station in order to produce a predicted water property

value for that station. The predictive power of the model was evaluated with the coefficient of determination (r^2_{jac}) between the recorded and the jackknife-estimated water property.

5.4. MERIS image

MERIS is a medium-spectral resolution, imaging spectrometer operating in the solar reflective spectral range. It forms part of the of ESA's environmental research satellite ENVISAT-1. MERIS has a swath width of 1150 km, measuring the solar radiation reflected by the Earth in 15 spectral bands, from about 412.5 nm to 900 nm (ESA 1996: http://envisat.esa.int/instruments/meris/). Because of the wide instrument field of view (68.5°), spatial sampling varies in the across track direction, between 0.26 km at nadir and 0.39 km at swath extremities. The spatial resolution over the Bay of Biscay is 260 m x 300 m. The MERIS overpass time for central Europe is between 9:30 and 11:00 UTC, with a global coverage every 3 days.

The MERIS images of the corresponding dates to the oceanographic survey were 11, most of them affected by clouds and haze (7). Thus, the MERIS image less affected by clouds, which was acquired on the 20th of May 2008, was selected and downloaded using the Eolisa interactive tool. The geo-located and atmospherically-corrected reflectance MERIS full resolution (FR) product (level 2) was used. This image was used to produce a chlorophyll-*a* map using the BEAM 4.6 program, available from: http://www.brockmann-consult.de/beam/.

There was a maximum time-lag (i.e. absolute time difference between *in-situ* and satellite measurements) lower than 5 hours. On the day the image was acquired, 6 stations were sampled. The MERIS bands used were 4 (510 nm) and 5 (560 nm). The reflectance band values were divided by π since the MERIS reflectance is defined as (ESA 2006):

$$\rho_w = \pi \frac{L_w(\lambda)}{E_s(\lambda)}$$

Where E_s, is the downwelling irrandiance and L_w the water-leaving radiance (after removal of air-sea interface reflection).

The algorithm with the best correlation between the band ratios and Chla, was represented using the "bandmath" application of the program. Cloud and land masks, provided by the level 2 product, were applied.

6. Results

The 68 stations sampled during the Bioman survey showed temperatures ranging between 15.0 and 17.8 ºC, with salinities between 25.3 and 35.7. Water masses influenced by river discharges were colder (15.0 ºC) and had lower salinities (25.3), than marine (offshore) water masses. The Chla ranged between 0.1 and 9.0 $\mu g.l^{-1}$. Most of the samples had concentrations below 4 $\mu g.l^{-1}$, except for 5 samples. SPM values ranged between 0.68 and 14.15 $mg.l^{-1}$, although most recorded values were below 3 $mg.l^{-1}$ and only a few above. Turbidity ranged between 0.01 and 7.50 NTU, with most of them being below 3 NTU. CDOM data ranged between 0.1 and 1 m^{-1} (Absorbance at 460 nm), where most recorded absorbances were below 0.4 m^{-1}, except for 8 of the measurements.

Figure 3 shows the Rrs spectra of a subset of sampling stations, obtained at the sea water surface, during the survey. The spectral range shown in the Figure was limited to 450-750 nm, due to the high noise recorded at wavelengths below and above this range, when measurements were performed on the field. Three different types of spectra, corresponding to different water masses, could be distinguished: (1) oceanic waters (low Chla, low SPM, low CDOM) (2) plume influenced waters (High Chla, medium SPM, high CDOM); and (3) estuarine waters (low Chla, high SPM, high CDOM). The estuarine water spectrum in Figure 3 corresponds to the station located inside the Gironde estuary (Figure 2), with a salinity of 25.3. The oceanic water spectrum shows a peak emerging in the blue area around 450 nm, which decreases with higher wavelengths. With the increasing influence of river freshwater, a depression can be observed in the blue area of the spectrum around 450 nm, as well as a peak emerging between 500 and 600 nm. Both depressions and peaks are magnified with increasing Chla, SPM and CDOM. With increasing freshwater input from the river, the highest spectral peak shifted towards higher wavelengths. Also, a peak of lower magnitude appears around 670 and 700 nm (0.001-0.002 sr^{-1}).

(*Approximate location of Figure 3)

The band ratios obtained from the survey data were calculated and correlated to Chla (Table 1). The highest correlation is obtained between the log-transformed Rrs(510)/Rrs(560) ratio and the log-transformed Chla (r^2 = 0.764). However, when the highest SPM (14.15 $mg.l^{-1}$) is removed from the dataset, the r^2 value increased for all the correlations (Rrs510/560 = 0.808), indicating a negative effect of SPM concentration on the Chla algorithms (Figure 4). On the other hand, there is a slight decrease in the r^2 values when the 8 stations with the highest SPM values were removed (Table 1). In addition, when the 8 stations with the highest CDOM values were removed from the dataset (n=56), there is a significant increase in all of the band ratio correlations with Chla (Table 1). Once again, the best correlation was obtained with Rrs510/560 (r^2 = 0.827; r^2_{jac} =0.816).

(*Approximate location of Figure 4 and Table 1)

The algorithms tested (OC4, OC3M, OC4E, Chlor_a_3) presented lower r^2 values than the Rrs510/560 band ratio, with the best of the four being the one obtained with the OC4E algorithm (Table 2). Figure 5 shows the linear regression between Chla, estimated by the different algorithms, and *in-situ* Chla. Figure 4 represents the correlation between the *in-situ* and the predicted Chla, using the Rrs510/560 algorithm ($Chla = 10^{-1.432R + 0.388}$; where R = Log(Rrs510/Rrs560), and it is compared with the MERIS OC4E algorithm, adjusted to our dataset. The algorithms were calculated with the reflectance value at the central wavelength of the corresponding band. The calculations performed considering the wider bandwidths for SeaWiFS (20 nm), MODIS (20 nm) and MERIS (10 nm), did not improve significantly the resulting r^2 (increased by 0.03), so only the calculations performed with the central wavelengths are shown.

(*Approximate location of Figure 5 and Table 2)

The best estimation of Chla in the continental shelf of the Bay of Biscay was obtained with Rrs510/560 band ratio. Thus, we applied this relation to the unique MERIS image acquired with low cloud coverage (Figure 6) during the oceanographic survey (20th of May 2008).The biggest difference of estimated Chla obtained between the algorithm developed and the Chla measured *in-situ*, was of 1 $\mu g.l^{-1}$ and the smallest of 0.2 $\mu g.l^{-1}$. The biggest difference between the estimated Chla by the MERIS Algal I algorithm and the concentration measured *in-situ* was

of 2 µg.l^{-1} and the smallest of 0.2 µg.l^{-1}, and of 1.5 µg.l^{-1} and 0.2 µg.l$^{-1,}$ with the MERIS Algal II algorithm.

The chlorophyll map shows the areas with the highest Chla concentrations located close to the French coast and river mouths, corresponding with the brownish coloured water in the RGB image (Figure 2).
(*Approximate location of Figure 6)

7. Discussion

7.1. Spectral measurement procedure

The main advantages of the upwelling-radiance measuring platform (a stainless steel flotation device) developed, include: its relative lightness (it can be released easily overboard); its stability (the sensor is maintained at a fairly constant distance, just below the water surface, i.e. approx. 1 cm); and the fact that measurements are performed at nadir (perpendicular to the water surface). Because of the platform, the *in-situ* spectral sampling could be carried out rapidly and in a consistent manner, since the sensor is adjusted easily to the correct position and its stability is guaranteed by the design.

The consistency of the Rrs, derived from the radiance measurements of Chla (at sea surface under different meteorological conditions), together with the similarity to the reflectance spectral signatures obtained with semi-analytically modelled reflectance spectra (Morel and Maritorena 2001), show that the experimental protocol provides coherent results. Therefore, adoption of 'the below surface measurement method' was appropriate, in accordance of the conclusions of Froidefond and Ouillon (2005).

The spectral range of the HR4000CG radiance measurements was limited to 440-700 nm, due to the high background noise obtained beyond this spectral region on the field measurements. An anomalous peak appears around 430 nm, which cannot exist in nature, i.e. compared to published spectra (Schalles 2006). This is due probably to an instrumental error, as it can be observed in all the reflectance spectra. There is also a peak at 760 nm, which corresponds to the oxygen absorption feature (Schott 1997). The appearance of this peak in reflectance spectra is due to the fact that both radiance and irradiance measurements were not performed simultaneously, as the absorption by atmospheric oxygen should not be seen in aquatic spectra. Most remote sensing Chla algorithms use wavelengths within the 440-700 nm range; therefore, they are not affected by these anomalous peaks. Statistically, significant correlations can be used later for empirical algorithm development, at a regional scale. In future, simultaneous measurements in the field, with other spectrometers, could be used as complementary validation of the spectral signatures obtained.

7.2. Estimation of the Chla

The spectral signatures obtained for the different types of waters coincide with the spectral signature presented by Schalles (2006). For instance, from the water samples collected, a shift of the highest peak towards higher wavelengths (from 500 nm, towards 600 nm) can be noted with increasing river load influence. Interestingly, it has been reported that in sediment laden waters, there is an increase in reflectance that affects the whole of the spectrum (Morel and Bélanger 2006). However, the green part of the spectrum (510-570 nm) is heightened anomalously, when compared to Case 1 waters with the same Chla (Bricaud and Morel 1987). Spectral signatures acquired during the survey show also a depression increase, with increasing

Chla in the blue area of the spectrum (440 nm); this corresponds to the maximum absorption wavelength of chlorophyll-*a* (Morel and Prieur 1977, Sathyendranath *et al*. 1987). In the range near to 560 nm, absorption by chlorophyll-*a* is weak so there is a noticeable increase in reflectance, as a result of the increase in backscattering (Morel 2006). In fact, the phytoplankton absorption minimum is considered to be around 550-560 nm, by remote sensors such as SeaWiFS or MODIS (IOCCG 1998).

Passive sun-induced fluorescence is detected in reflectance spectra (Morel and Prieur 1977), since fluorescence provides a specific signal issued by chlorophyll-*a* within the antenna of Photosystem II. The fluorescence intensity is quantified with a peak emerging in the 683 nm channel (red), with two depressions at either side of the peak. Chlorophyll-*a* fluorescence overlaps with a strong NIR elastic scattering peak (Gilerson *et al*. 2007). The decrease in algal absorption, the increase in water absorption, and the scattering of phytoplankton cell structures are located in the same spectral zone as the fluorescence emission (Dall'Olmo *et al*. 2005). In highly turbid and productive waters (Chla 9 to 77.4 $\mu g.l^{-1}$; SPM: 7 to 65 $mg.l^{-1}$dry wt; CDOM absorption at 440 nm 0.20 to 2.50 m^{-1}), absorption by pigments is minimal. Gitelson *et al.* (2007) showed that the position of the reflectance peak shifted towards longer wavelengths, with increasing Chla (from 688 nm when Chla was 9 $\mu g.l^{-1}$, to about 706 nm for Chla above 70 $\mu g.l^{-1}$). However, they also showed that Chla was poorly related to peak magnitude (responsible for only 2% of peak magnitude variation), suggesting that scattering by inorganic and non-living organic suspended matter controlled mainly reflectance in this spectral region. Our dataset included samples collected in waters were concentrations of inorganic and non-living suspended matter was low, with phytoplankton being the optically-dominant water component. There could be a possibility of fluorescence being observed in some of these spectra. However, the interpretation of fluorescence, in terms of phytoplanktonic biomass, is difficult. Essentially, the fluorescence signal depends not only upon the chlorophyll-*a* concentration itself, but also upon the intensity of the excitation, and on the fluorescence quantum yield, whose predictability is still questionable (Morel 2006).

The analysis of *in-situ* spectral signatures and the biogeochemical measurements acquired over the shelf of the Bay of Biscay has revealed a strong relationship between Chla and Rrs. The highest correlation values obtained correspond to band ratios used in the SeaWiFS OC4, the MERIS OC4E and the MODIS OC3 algorithms. Hence, a polynomial, potential or exponential fit to these band ratios, with Chla, could be used as an algorithm for the retrieval of Chla in the waters surveyed. In contrast, when validating the dataset with the algorithms used by the remote sensors with the Jackknife procedure, the resulting r^2 values were lower than the ratios (Tables 1 and 2).

The correlation between Chla and the band ratios Rrs510/Rrs560, Rrs510/Rrs555, Rrs490/Rrs560 and Rrs488/Rrs551 improve when the station with the highest SPM (Station 42: 14.15 $mg.l^{-1}$) is removed from the data set, whilst all others sampling stations presented SPM < 5.2 $mg.l^{-1}$. This pattern suggests the influence of SPM, on these correlations. The increase in particulate matter would have caused the ratio-Chla relationship at this station to be different with respect to the other stations. Station 42 was located inside of the Gironde estuary (Le Verdon), where SPM surface concentrations of between 35 and 2072 $mg.l^{-1}$ have been reported during summer time (Doxaran *et al*. 2002). Conversely, when the 8 stations with the highest SPM concentrations (<2.8 $mg.l^{-1}$) were removed, the correlations again decreased (r^2 = 0.74, for the Rrs510/560). This suggests that there is only the effect of highly turbid waters on the relationship. When the 8 stations with the highest CDOM absorbance (>0.4 m^{-1}) were removed from the dataset, there was a significant increase of the r^2 values of all the ratios. The highest

relationship was found also with Rrs510/R560 (r^2_{jac} = 0.816); this implies that CDOM is affecting all of the bands considered, i.e. channels between 443 and 560.

Thirty-five stations of our data set had a dominant phytoplankton component (High Chla, low SPM and CDOM), while 29 of the stations were located in waters where Chla was not the dominant constituent (4 stations where discarded). CDOM, in these 29 stations, presents values above 0.4 m^{-1} and 2 stations showed SPM values above 5 $mg.l^{-1}$. Considering the IOCCG (2000) optical classification of water bodies, 35 stations would correspond to Case 1 waters and 29 to Case 2 On the other hand, most of the stations with dominant Chla (26) have concentrations of below 1 $\mu g.l^{-1}$. The relationship derived between stations with Chla lower than 1 $\mu g.l^{-1}$ and Rrs510/560, resulted in an r^2 of 0.424; this suggests that there might be limitations in estimating Chla, based upon reflectance with the spectrometer (field or satellite) in waters with low Chla, as has happened with already-established algorithms (Hooker and McClain 2002). Water bodies where the phytoplankton component is not dominant (SPM or CDOM are dominant), show an even lower relationship with this band ratio (r^2 = 0.2).

In areas where phytoplankton dominates the water colour, whilst the scattering and absorbing components of seawater co-vary with Chla, blue-green band-ratio algorithms are often successful, as phytoplankton absorbs more blue light than green. However, the precision of these algorithms can diminish when environmental conditions differ from those representative of the data set analysed, to derive empirically the covariance relationships (Carder *et al*. 2003). Thus, chlorophyll-*a* absorption by phytoplankton can change depending upon the species, nutrient concentration or lighting conditions. In Case 2 waters, substances that do not co-vary with Chla, change the water optical conditions. This causes inaccuracies in the retrieval of pigment concentration on the basis of satellite imagery (Carder *et al*. 1991). The variability of in-water constituents, due to environmental changes such as upwelling currents waters or river run-off input, needs to be considered in algorithm parameterisation. Therefore, a large data set needs to be gathered, in order to develop robust empirical algorithms for the continental shelf of the Bay of Biscay, which take into account seasonal and local variations. In particular, chlorophyll-a algorithms for turbid coastal waters might incorporate the green to red band ratio, as those developed by Dall'Olmo and Gitelson (2005) and Gitelson *et al.* (2007).

Field spectrometers have been used successfully for Chla retrieval from reflectance spectra (Gitelson *et al*. 1999, Tzortziou *et al.* 2007), the development of bio-optical Chla estimation (O'Reilly 1998), as well as validation of remote sensing data products (Werdell and Bailey 2005). In fact, the SeaWiFS and MODIS remote sensors have been vicariously calibrated with *in-situ* spectroradiometric measurements by means of the Marine Optical Buoy program (MOBY) (Bailey *et al*. 2008). MOBY included a radiometric buoy deployed in clear, deep ocean waters off Hawaii, measuring the upwelling radiance and downwelling irradiance, at three levels below the ocean surface. Dall´Olmo and Gitelson (2005), Dall'Olmo *et al*. (2003, 2005), and Gitelson *et al*. (2007, 2008) used reflectance spectra, obtained with the previous model (the Ocean optics USB2000), to the HR4000CG spectrometer, with a similar methodology, to evaluate the extent to which reflectance ratios could be applied to remote sensors to estimate Chla in turbid waters. Within this context, the HR4000CG spectrometer, the platform developed and the protocol established, could be used as a tool to retrieve Chla from normalized water-leaving satellite images obtained with remote sensors, such as MODIS and MERIS. This tool could be used in the assessment of the Bay of Biscay continental shelf water quality.

The MERIS RGB image, corresponding to the oceanographic survey, illustrates the influence of coastal areas and river plumes; waters appear greener and darker than oceanic waters and the colours match the estimated high Chla (Figure 6). The effect of coastal CDOM

and SPM could have influenced also the Chla estimation using the algorithm developed here, since it has been found that there is an effect of these parameters on the Chla-ratio relationship.

This is a first approach towards the development of a regionally-parameterized algorithm, on the basis of the field spectrometer spectra and MERIS images. In order to reach this objective, it is necessary to use a larger data set together with a more extensive study of the empirical relationships existing between water parameters and 'apparent optical properties'. Ongoing research in specific areas (Northern Spain and Adour river mouth) will permit the enlargement of the data set for the development of more robust relationships.

8. Conclusions

The custom-built platform developed, the stainless steal flotation device, and the protocol established for the HR4000CG spectrometer, have been proved to be useful tools to acquire reflectance spectra, at the sea surface and estimate Chla with MERIS images. The spectral signatures acquired are consistent with reported algal culture reflectance spectra (Gitelson *et al.* 1999) and reflectance spectra acquired at sea (Morel 2006). As such, a depression in the blue part of the spectra and a red peak near 675 nm, with increasing Chla, can be noted. Spectral classification of different water bodies influenced by river freshwater was possible; and these corresponded with published spectra in the literature (Schalles 2006). Correlations between reflectance ratios used by SeaWiFS and MERIS algorithms and Chla are statistically significant, with the best correlation found with the Rrs(510)/Rrs(560) ratio (r^2_{jac} = 0.681). High content in CDOM (>0.4 m^{-1}) and SPM (>2.8 $mg.l^{-1}$) influenced this relationship, although yellow substances could be noted to have a stronger effect (r^2_{jac} (CDOM<0.4 m^{-1}) = 0.816, r^2_{jac} (SPM< 2.8 $mg.l^{-1}$) = 0.742). This is a preliminary approach towards the development of a regionally-parameterized algorithm to estimate Chla with the MERIS sensor for the continental shelf of the Bay of Biscay.

Acknowledgements

This research was supported by the Ministry of Education and Science (Spanish Government, Ref.: ESP2006-10411) and the Funds for Aquitania–Euskadi cooperation (Basque Government). S. Novoa benefits from a PhD scholarship granted by the Fundación de Centros Tecnológicos Iñaki Goenaga. MERIS data were provided by the European Space Agency (ESA Category-1 scheme, proposal nr. 5395). The authors wish to acknowledge: the contribution of Dr. J. Franco for his valuable technical support, on chlorophyll estimation; to M. Santos, coordinator of 2008 BIOMAN campaign; and to Dr. A. Borja and the Professor Michael Collins (School of Ocean and Earth Science, University of Southampton and AZTI-Tecnalia) for their useful comments. This is the contribution XXX from the AZTI-Technalia Marine Research Division.

References

APHA, AWWA and WPCF, 1989, *Standard Methods for the Examination of Water and Wastewater.* (Washington, DC: American Public Health Association).

BAILEY, S.W., HOOKER, S. B., ANTOINES, D., FRANZ, B.A and WERDELL, P. J., 2008, Sources and assumptions for the vicarious calibration of ocean colour satellite observations. *Applied Optics*, **47**, pp. 2035-2045.

BØGESTRAND, J., KRISTENSEN, P. and KROVANG, B., 2005, Source apportionment of nitrogen and phosphorus inputs into the aquatic environment. *European Environmental Agency* (EEA), **7**, pp. 1-48.

BORJA, A., FRANCO, J., VALENCIA, V., BALD, J., MUXICA, I., BELZUNZE, M.J. and SOLAUN, O., 2004, Implementation of the European water framework directive from the Basque country (northern Spain): a methodological approach. *Marine Pollution Bulletin*, **48**, pp. 209–218.

BRICAUD, A. and MOREL, A., 1987, Atmospheric corrections and interpretation of marine radiances in CZCS imagery: use of a reflectance model. *Oceanologica Acta*, N°SP, pp. 33-50.

BURNHAM, K. P. and ANDERSON, D. R. (Eds.), 2002, *Model selection and multimodel inference: a practical information-theoretic approach: 2nd Edition*, pp. 488 (New York: Springer-Verlag)

CARDER, K.L., HAWES, K.A., BAKER, R.C., SMITH, R.G., STEWARD, R.J. and MITCHELL, B.G., 1991, Reflectance model for quantifying chlorophyll-*a* in the presence of productivity degradation products, *Journal of Geophysical Research,* **96**, pp. 20599–20611.

CARDER, K. L., CHEN, F. R., LEE, Z. P. and HAWES, S. K., 1999, Semi-analytic Moderate-Resolution Imaging Spectrometer algorithms for chlorophyll-a and absorption with bio-optical domains based on nitrate-depletion temperatures. Journal of Geophysical Research, 104, pp. 5403-5421.

CARDER, K. L., CHEN, F. R., LEE, Z. P., HAWES, S. K. and CANNIZARO, J.P., 2003, ATBD 19: Case 2 Chlorophyll-*a*. MODIS Ocean Science Team Algorithm Theoretical Basis Document, pp. 1-67.

DALL'OLMO, G., GITELSON, A. A. and RUNDQUIST, D. C., 2003, Towards a unified approach for remote estimation of chlorophyll-*a* in both terrestrial vegetation and turbid productive waters. *Geophysical Research Letters,* **30**, pp. 1938-1941.

DALL'OLMO, G. and GITELSON, A. A., 2005, Effect of bio-optical parameter variability on the remote estimation of chlorophyll-*a* concentration in turbid productive waters: experimental results. *Applied optics*, **44**, pp. 412-422.

DALL'OLMO, G., GITELSON, A. A., RUNQUISTA, D. C., LEAVITTA, B., BARROW, T. and HOLZ, J.C., 2005, Assessing the potential of SeaWiFS and MODIS for estimating chlorophyll concentration in turbid productive waters using red and near-infrared bands. *Remote Sensing of Environment*, **96**, pp. 176-187.

DARECKI, M. and STRAMSKI, D., 2003, An evaluation of MODIS and SeaWiFS bio-optical algorithms in the Baltic Sea. *Remote Sensing of Environment*, **89**, pp. 326-350.

DOMINGUES, R.B., BARBOSA, A. and GALVÃO, H., 2008, Constraints on the use of phytoplankton as a biological quality- element within the Water Framework- Directive in Portuguese waters. *Marine Pollution Bulletin,* **56,** pp. 1389–1395.

DEVLIN, M., BEST, M. and HAYNES, D., 2007, Implementation of the Water Framework Directive in European marine waters. *Marine Pollution Bulletin*, **55**, pp. 1-2.

DOXARAN, D., FROIDEFOND, J.M., LAVENDER, S. and CASTAING, P., 2002, Spectral signature of highly turbid waters: Application with SPOT data to quantify suspended particulate matter concentrations. *Remote Sensing of Environment*, **81**, pp. 149–161.

DOXARAN, D. FROIDEFOND, J.M., CASTAING, D. and BABIN, M., 2009, Dynamics of the turbidity maximum zone in a macrotidal estuary (the Gironde, France): Observations from field and MODIS satellite data. *Estuarine, Coastal and Shelf Science,* **81,** pp. 321–332.

ESA. European Space Agency, 2006. *MERIS Product Handbook*, **2.1**., pp. 70.

FROIDEFOND, J.M., LAVENDER, S., LABORDE, P., HERBLAND, A. and LAFON, V., 2002, SeaWiFS data interpretation in a coastal area in the Bay of Biscay. *International Journal of Remote Sensing*, **23**, pp. 881-904.

FROIDEFOND, J.M. and OUILLON, S., 2005, Introducing a mini-catamaran to perform reflectance measurements above and below the water surface. *Optics Express*, **13**, pp. 926-936.

GARCIA-SOTO, C. and PINGREE, R.D., 2009, Spring and summer blooms of phytoplankton (SeaWiFS/MODIS) along a ferry line in the Bay of Biscay and western English Channel. *Continental Shelf Research*, **29**, pp. 1111-1122.

GILERSON, A., ZHOU J., HLAING, S., IOANNOU, I., SCHALLES, J., GROSS, B., MOSHARY, F., and AHMED, S., 2007, Fluorescence component in the reflectance spectra from coastal waters. Dependence on water composition. *Optics Express*, **15**, pp. 15702-15721.

GITELSON, A. A., SCHALLES, J.F., RUNQUIST, D.C., SCHIEBE, F.R. and YACOBI, Y. Z., 1999, Comparative reflectance properties of algal cultures with manipulated densities. *Journal of Applied Phycology,* **11**, pp. 345–354.

GITELSON, A. A., SCHALLES, J.F. and HLADIK, C.M., 2007, Remote chlorophyll-*a* retrieval in turbid, productive estuaries: Chesapeake Bay case study. *Remote Sensing of Environment*, **109**, pp. 464–472.

GITELSON, A. A., DALL'OLMO, G., MOSES, W., RUNQUIST, D. C., BARROW, T., FISHER, T.R., GURLIN, D. and HOLZ, J., 2008, A simple semi-analytical model for remote estimation of chlorophyll-*a* in turbid waters: Validation. *Remote Sensing of Environment*, **112**, pp. 3582-3593.

GOHIN, F., SAULQUIN, B., OGER-JEANNERET, H., LOZAC´H, L., LAMPERT, L., LEFEBVRE, A., RIOU, P. and BRUCHON, F., 2008, Towards a better assessment of the

ecological status of coastal waters using satellite-derived chlorophyll-*a* concentrations. *Remote Sensing of Environment*, **112**, pp. 3329–3340.

GONZÁLEZ, M., URIARTE, A., FONTÁN, A., MADER, J. and GYSSELS, P., 2004, Marine dynamics. *Oceanography and Marine Environment of the Basque Country*, pp. 133-157. Borja, A., Collins, M. (Eds.) (Elsevier Oceanography Series).

GORDON, H.R. and MOREL, A.Y., 1983, *Remote Assessment of Ocean Colour for Interpretation of Satellite Visible Imagery: A Review*. (New York: Springer-Verlag).

GUILLAUD, J.F., AMINOT, A., DELMAS, D., GOHIN, F., LUNVEN, M. LABRY, C. and HERBLAND, A., 2008, Seasonal variation of riverine nutrient inputs in the northern Bay of Biscay (France), and patterns of marine phytoplankton response. *Journal of Marine Systems,* **72**, pp. 309-319.

HELLWEGER, F.L., SCHLOSSER, P., LALL U. and WEISSEL, J.K., 2004, Use of satellite imagery for water quality studies in New York Harbor. *Estuarine, Coastal and Shelf Science*, **61**, pp. 437–448.

HOOKER, S.B. and MCCLAIN, C.R., 2000, The calibration and validation of SeaWiFS data. *Progress in Oceanography*, **45**, pp. 427-465.

IOCCG, 1998, Minimum Requirements for an Operational Ocean-Colour Sensor for the Open Ocean. *Reports of the International Ocean Colour Coordinating Group*, 46 pp. (Dartmouth, Canada: IOCCG Project Office).

IOCCG, 2000, Remote Sensing of Ocean Colour in Coastal, and Other Optically-Complex, Waters. *Reports of the International Ocean-Colour Coordinating Group,* **3**, IOCCG. Sathyendrath, S.(ed.), pp. 144.

JEFFREY, S.W. and HUMPHREY, G. F., 1975, New Spectrophotometric equations for determining chlorophylls a, b, c1 and c2 in higher plants, algae, and natural phytoplankton. *Biochemical Physiology Pflanz*, **167**, pp. 191-194.

LEE, Z. and HU, C., 2006, Global distribution of Case-1 waters: An analysis from SeaWiFS measurements. Remote Sensing of Environment, **101**, pp. 270 – 276

LONGHURST, A., 1998, *Ecological Geography of the Sea,* pp. 385 (San Diego, CA: Academic press).

MILLER, P., SHUTLER, J., MOORE, G. and GROOM, S., 2006, SeaWiFS discrimination of harmful algal bloom evolution. *International Journal of Remote Sensing*, **27**, pp. 2287–2301.

MOBLEY, C. D., 1994*, Light and Water: Radiative Transfer in Natural Waters,* pp. 592 (San Diego, CA: Academic press).

MOBLEY, C. D., 1999, Estimation of the remote-sensing reflectance from above-surface measurements. *Applied Optics*, **38**, pp.7442–7455.

MOBLEY, C. D., STRAMSKI, D., BISSET, W. P. and BOSS, E., 2004, Optical modeling of ocean waters: Is the Case 1 –Case 2 classification still useful? *Oceanography*, **17**, pp. 60–67.

MOREL, A., 1988, Optical modeling of the upper ocean in relation to its biogenous matter content (case 1 water). *Journal of Geophysical Research*, **93**, pp. 749-768.

MOREL, A., 2006, Meeting the Challenge of Monitoring Chlorophyll in the Ocean from Outer Space. *Chlorophylls and Bacteriochlorophylls: Biochemistry, Biophysics, Functions and Applications*, Grimm, B., Porra, R.J., Rüdiger, W., Scheer, H. (Eds.), pp. 521–534. (The Netherlands: Springer).

MOREL, A. and PRIEUR, L., 1977, Analysis of variations in ocean colour. *Limnology and Oceanography*, **22**, pp. 709-722.

MOREL, A., AHN, Y., PARTENSKY, F., VAULOT, D. and CLAUTRE, H., 1993, Prochlorococcus and Synechococcus: a compartive study of their size, pigmentation and related optical properties. *Journal of Marine Research,* **51**, pp. 617-649.

MOREL, A. and MARITORENA, S., 2001, Bio-optical properties of oceanic waters: A reappraisal. *Journal of Geophysical Research*, **106**, pp. 7163–7180.

MOREL, A. and BÉLANGER, S., 2006, Improved detection of turbid waters from the ocean colour sensors information. *Remote sensing of the environment*, **102**, pp. 237-249.

MUELLER, J.L., 2002, Overview of measurement and data analysis protocols. *Ocean Optics Protocols for Satellite Ocean-Color Sensor Validation.* Mueller, J.L. and Fargion, G.S (Eds.). Revision 3, **1**, pp. 136 (NASA Tech. Memo. 210004).

OCEAN OPTICS INC., 2001-2006, High-Resolution Fiber Optic Spectrometers HR4000 / HR4000CG-UV-NIR. *Installation and Operation Manual*, pp 1-40. Document Number 210-00000-000-02-1006.

OCEAN OPTICS INC., 1999-2007, Spectrasuite manual. *Spectrometer Operating Software Installation and Operation Manual*, pp. 1-154 (Document Number 000-20000-300-02-0307).

O'REILLY, J.E., MARITORENA, S., MITCHELL, B.G., SIEGEL, D.A., CARDER, K.L., GARVER, S. A., KAHRU, M. and MCCLAIN, C., 1998, Ocean colour chlorophyll algorithms for SeaWiFS. *Journal of Geophysical Research*, **103,** pp. 24937–24953.

ORIVE, E., FRANCO, J., DE MADARIAGA, I., and REVILLA, M., 2004, Bacterioplankton and phytoplankton communities. *Oceanography and Marine Environment of the Basque Country*. Borja, A., Collins, M. (Eds), pp 367- 393. (Elsevier Oceanography Series)

OUILLON, S. and PETRENKO, A., 2005, Above-water measurements of reflectance and chlorophyll-*a* algorithms in the Gulf of Lions, NW Mediterranean Sea. *Optics Express,* **13**, pp. 2531-2548.

PÉREZ PUEBLA, F., 2009*, El riesgo de tormenta* (The Storm risk). Asociación Meteorológica Española.

PETUS, C., CHUST, G., SAGARMINAGA, Y. and FROIDEFOND, J.M., 2008, Estimating turbidity indicators and total suspended matter in the Bay of Biscay using MODIS 250-m imagery. *Revista de Investigación Marina*, **3**, pp. 180-181.

PRIEUR, L., and SATHYENDRANATH, S., 1981, An optical classification of coastal and oceanic waters based on the specific spectral absorption curves of phytoplankton pigments, dissolved organic matter, and other particulate materials. *Limnology and Oceanography*, **26**, pp. 671–689.

REVILLA, M., FRANCO, J., BALD J., BORJA, A., LAZA, A., SEOANE, S. and VALENCIA, V., 2009, Assessment of the phytoplankton ecological status in the Basque coast (northern Spain) according to the European Water Framework Directive, *Journal of Sea Research*, **61**, pp. 60–67

SATHYENDRANATH, S., LAZZARA, L. and PRIEUR, L., 1987, Variations in the spectral values of specific absorption of phytoplankton. *Limnology and Oceanography,* **32**, pp. 403–415.

SATHYENDRANATH, S., HOGE, F. E., PLATT, T. and SWIF, R. N., 1994, Detection of phytoplankton pigments from ocean colour: Improved algorithms. *Appl. Optics*, **33**, pp. 1081-1089.

SCHALLES, J. F., 2006, Optical Remote Sensing techniques to estimate Phytoplankton Chlorophyll a concentrations in coastal waters with varying suspended matter and CDOM concentrations. *Remote Sensing of Aquatic Coastal Ecosystem Processes: Science and Management Applications*. Chapter 3. L. L. Richardson and E. F. LeDrew, Springer (Eds.).

SCHILLER, H. and DOERFFER, R., 1999, Neural network for emulation of an inverse model – operational derivation of Case II water properties from MERIS data. *International Journal of Remote Sensing*, **20**, pp. 1735–1746.

SCHOTT, J.R., 1997, *Remote Sensing: The Imaging Chain Approach*, pp. 225 (Oxford University Press)

TZORTZIOU, M., SUBRAMANIAM, A., HERMAN, J. R., GALLEGOS, C.L., NEALE, P. J. and HARDING, L. W. Jr., 2007, Remote sensing reflectance and inherent optical properties in the mid Chesapeake Bay. *Estuarine, Coastal and Shelf Science*, **72**, pp. 16-32.

VARELA, M., 1996, Phytoplankton ecology in the Bay of Biscay. *The European anchovy and its environment.* Palomera, I., Rubiés, P. (Eds.), *Scientia Marina,* **60**, pp. 45-53.

WERDELL, P. J. and BAILEY, S. W., 2005, An improved *in-situ* bio-optical data set for ocean colour algorithm development and satellite data product validation. *Remote Sensing of Environment*, **98**, pp. 122-140.

ZAINUDDIN, M., KIYOFUJI, H., SAITOH, K. and SAITOH S., 2006., Using multi-sensor satellite remote sensing and catch data to detect ocean hot spots for albacore (Thunnus alalunga) in the northwestern North Pacific. *Deep Sea Research Part II: Topical Studies in Oceanography*, **53**, pp. 419-431.

VENABLES, W.N. and SMITH, D.M., 2007, R development core team. Notes on r a programming environment for data analysis and graphics, 2.6.1 version. *An introduction to R*, pp. 94.

Web pages:

CANTABRIAN HIDROGRAPHYCAL CONFEDERATION:
http://www.chcantabrico.es/index.php

Tables

Table 1. Band ratios and Chla with corresponding r^2, P-values and Jackknife validation r^2 values.

	All data n=64			Samples with CDOM>0.4 m^{-1} n=56			Samples with SPM>2.8 $mg.l^{-1}$ n=56		
Band ratio	r^2 Chla vs. Ratio	P-value	Jackknife validation r^2	r^2 Chla vs. Ratio	P-value	Jackknife validation r^2	r^2 Chla vs. Ratio	P-value	Jackknife validation r^2
443/555	0.498	6.23E-10	0.454	0.618	3.12E-12	0.595	0.613	2.70E-12	0.584
490/555	0.393	1.37E-07	0.345	0.441	4.77E-08	0.408	0.371	6.04E-07	0.333
510/555	0.75	<2.2e-16	0.66	0.813	<2.2e-16	0.801	0.736	<2.2e-16	0.721
490/550	0.395	1.29E-07	0.313	0.437	5.68E-08	0.408	0.368	6.95E-07	0.326
443/550	0.492	8.76E-10	0.442	0.620	2.64E-12	0.599	0.579	1.52E-11	0.557
443/560	0.495	7.46E-10	0.409	0.632	1.19E-12	0.612	0.495	1.76E-09	0.435
490/560	0.719	<2.2e-16	0.666	0.809	<2.2e-16	0.798	0.723	2.45E-16	0.708
510/560	0.764	<2.2e-16	**0.681**	0.827	<2.2e-16	**0.816**	0.756	<2.2e-16	**0.742**
443/551	0.694	<2.2e-16	0.437	0.629	1.47E-12	0.609	0.561	4.38E-11	0.532
488/551	0.706	<2.2e-16	0.672	0.804	<2.2e-16	0.792	0.737	<2.2e-16	0.722

Table 2. Chla algorithms for different sensors tested for the Bay of Biscay *in-situ* acquired data and resulting jackknife validation r^2 values.

Sensor	Equation	Maximum ratio value (R)	Jackknife validation r^2
MODIS/OC3M	$C = 10^{(0.2830 - 2.753R + 1.457R^2 - 0.659R^3 - 1.403R^4)}$	(443,490)/550	0.546
MERIS OC4E	$C = 10^{(0.368 - 2.814R + 1.456R^2 - 0.768R^3 - 1.292R^4)}$	(443,490,510)/560	0.587
SeaWiFS/OC4 v4	$C = 10^{(0.366 - 3.067R + 1.930R^2 + 0.649R^3 - 1.532R^4)}$	(443;490;510)/555	0.558
Carder MODIS (Chlor_a_ 3)	$C = 10^{(0.3147 - 2.859R + 2.007R^2 - 1.730R^3)}$	(443;488)/551	0.582
Adjusted OC4E	$C = 10^{(-0.215 - 0.2934R + 0.53R^2 + 0.141R^3 + 0.553R^4)}$	(443,490,510)/560	0.601

Figure Legends

Figure 1. Upwelling radiance measuring platform.

Figure 2. MERIS image (RGB composite) acquired on the 20th of May 2008 showing the stations where spectral and hydrological measurements were performed on the continental shelf of the Bay of Biscay.

Figure 3. Subset of samples showing Rrs and corresponding Chla for the Bay of Biscay, where three main water types can be distinguished spectrally. Rrs measurements were performed with a boxcar width of 8 plus an averaging of 10 adjacent channels was performed for display purposes.

Figure 4. Correlation between log-transformed Rrs(510)/(560) band ratio and Chla (in logarithmic scale). The OC4E algorithm adjusted to our dataset is shown in dashed lines.

Figure 5. Linear regression between *in-situ* Chla and algorithm estimated Chla: *(a)* OC3M, *(b)* OC4E, *(c)* OC4 and *(d)* Carder (Chlor_a_3).

Figure 6. Chlorophyll-*a* map generated using a MERIS image acquired during the survey (20th of May, 2008) and the linear relationship established between Chla and the Rrs510/560.

Figures

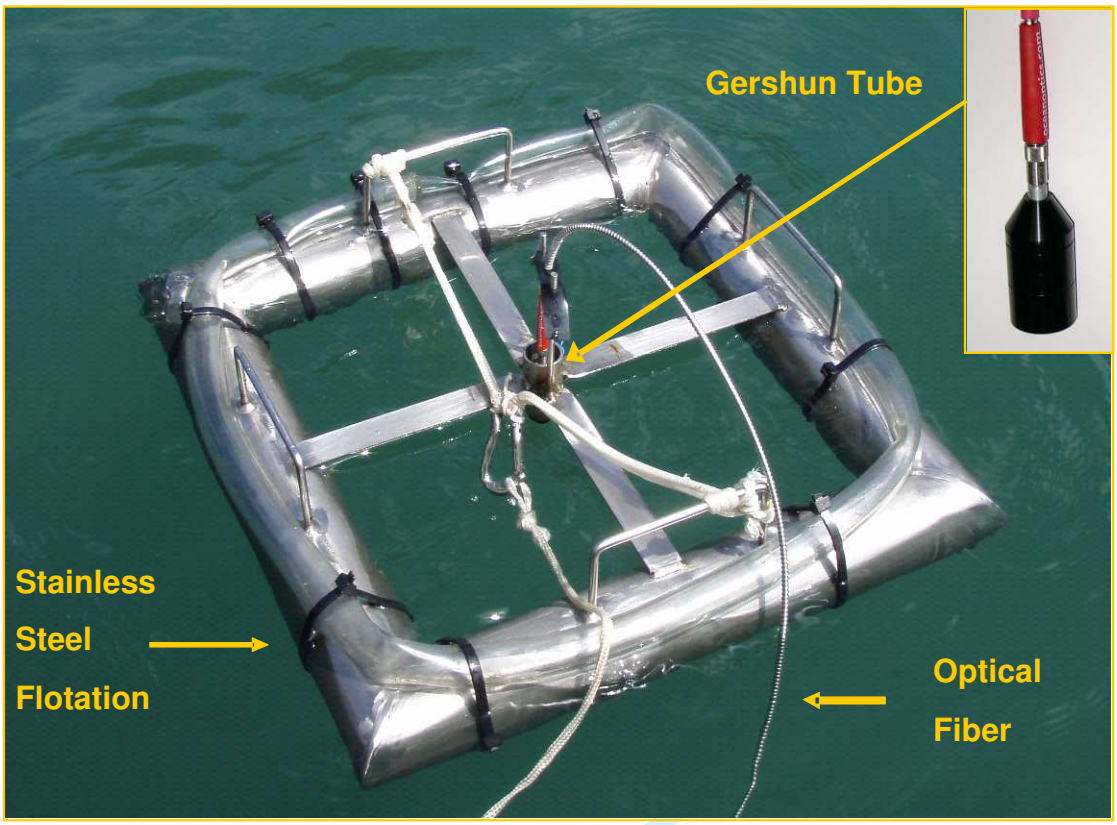

Novoa *et al.*: Figure 1

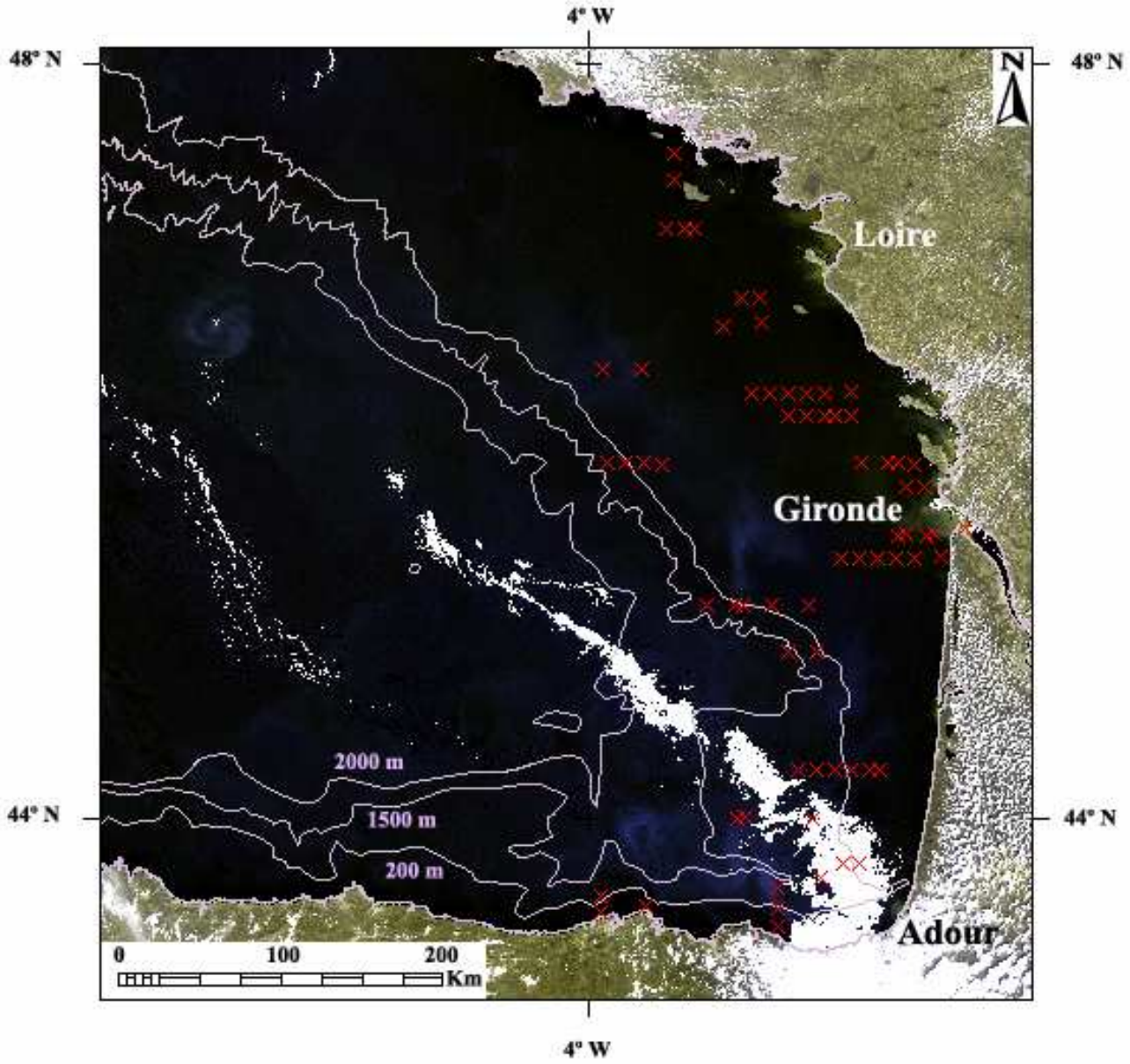

Novoa *et al.* : Figure 2

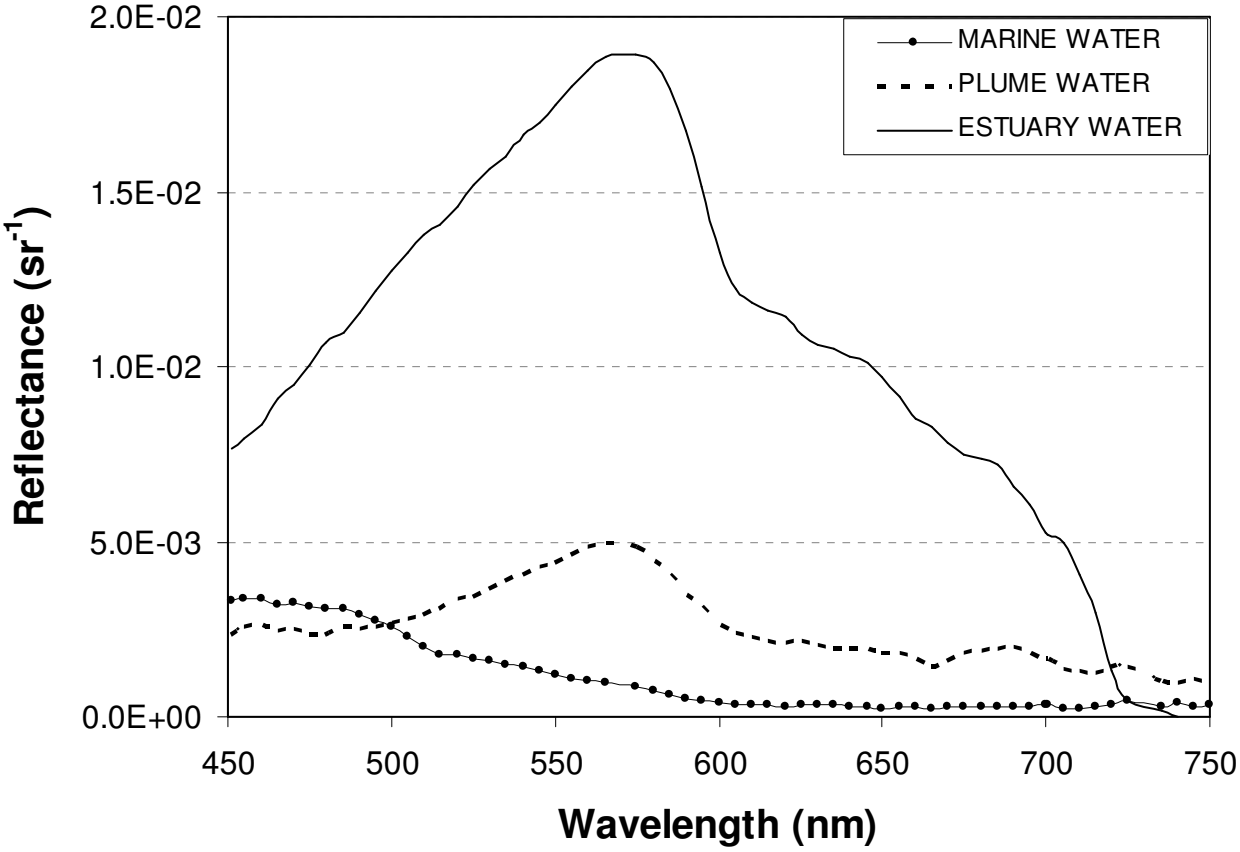

Novoa *et al.*: Figure 3

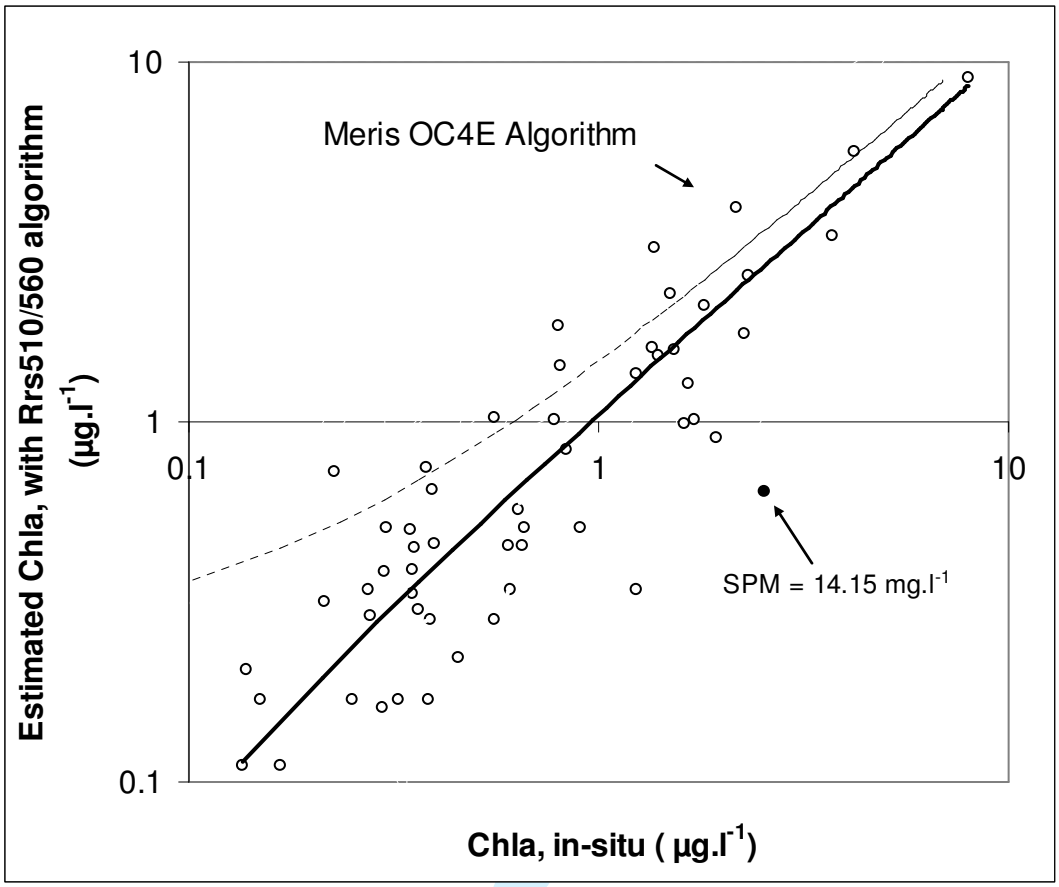

Novoa *et al.* : Figure 4

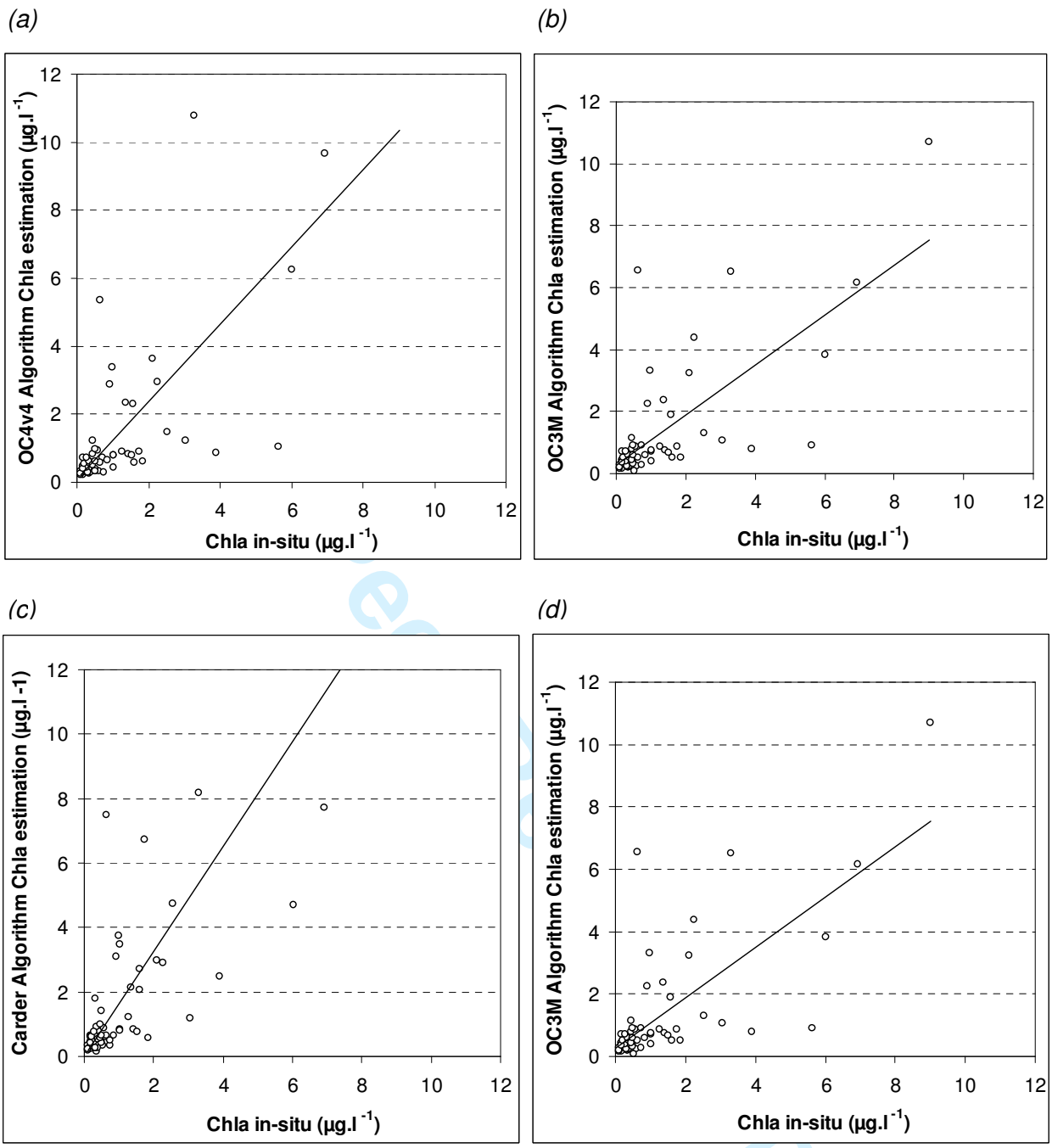

Novoa *et al.* : Figure 5

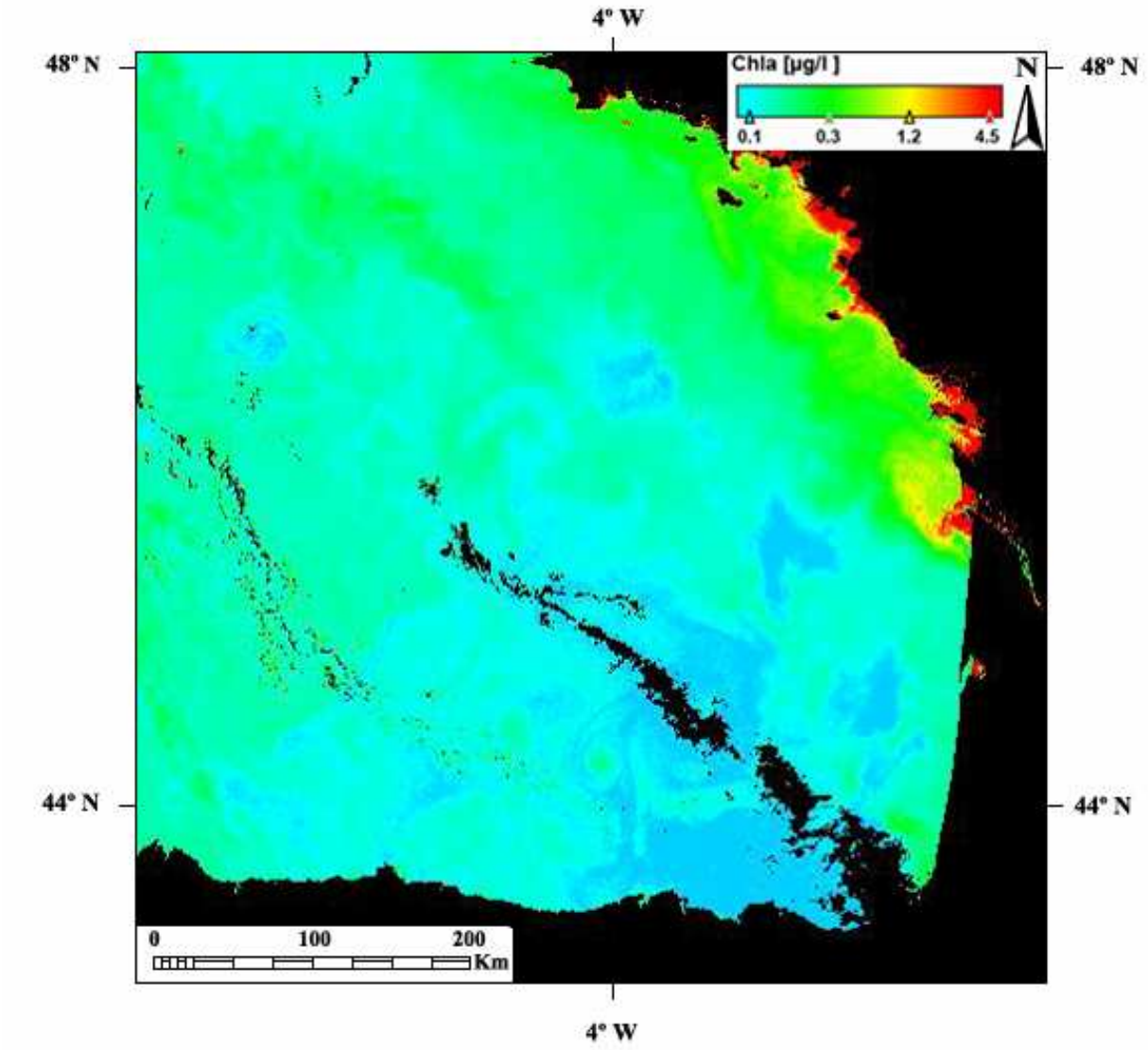

Novoa *et al.*: Figure 6